An Observer-Based Controller Design Method for Improving Air/Fuel Characteristics of Spark Ignition Engines

Seibum B. Choi and J. Karl Hedrick

***Abstract*—In the urban traffic mode, the engine is known to be operated mostly in a transient state. However, the wide operating range, the inherent nonlinearities of the induction process and the large modeling uncertainties make the design of the fuel-injection controller very difficult. Even though a sliding mode fuel-injection control method is in good agreement with the characteristics of the system, the unavoidable large time-delay between control action and measurement causes the problem of chattering. In this paper, an observer-based fuel-injection control algorithm is suggested for fast response and small amplitude chattering of the air-to-fuel ratio. The characteristics of the proposed controller are compared with those of other controllers. The proposed controller is simple enough for on-line computation and is implemented on an automotive engine using a PC-386. The simulation and the experimental results show that this algorithm reduces the chattering magnitude considerably while speeding up the transient response and is robust to modeling errors.**

***Index Terms*— Chatter free, delay effects, engines, fuel injection, observers.**

I. Introduction

THE method selected to meet the new exhaust emissions standards has been to use a catalytic converter that simultaneously oxidizes and reduces engine emissions. Unfortunately, the efficiency of the catalyst is very sensitive to the variation of the air-to-fuel (A/F) ratio. Therefore, it is apparent that the main issue of the control of the S.I. engine is to control the fuel-injector(s) to keep the A/F ratio close to stoichiometry (14.7) both in steady-state operation and during transients. The steady-state operation is trivial compared to the transient control, since all the air-induction dynamics and the fueling dynamics disappear at steady state. However, in the urban traffic mode, the engine is operated mostly in a transient condition, and this makes the design of a controller very difficult.

Manuscript received April 10, 1995. Recommended by Associate Editor, Associate Editor, B. Krogh.

S. B. Choi was with the University of California at Berkeley, Berkeley, CA 94720 USA. He is now with Varity Kelsey-Hayes, Livonia, MI 48150 USA.

J. K. Hedrick is with the Mechanical Engineering Department, University of California at Berkeley, Berkeley, CA 94720 USA. He is also with the California Path Research Center, Berkeley, CA 94720 USA.

Publisher Item Identifier S 1063-6536(98)03004-8.

Many of the current production fuel-injection controllers rely on open-loop feedforward control based on a lookup table with proportional plus integral (PI) feedback control [4]. However, building the table is a laborious process of calibration and tuning. Other linear control techniques, such as linear quadratic Gaussian (LQG), pole placement, and LQG/LTR have little advantage, since they need the output magnitude information while the control system is nonlinear and the sensor output is nearly binary [5], [13].

As a solution to this problem, a sliding mode fuel-injection control method was proposed [6], [8], [19]. This is an analytic design method and in good agreement with the binary nature of the oxygen sensor signal. However, in spite of many merits, this method has the problem of large amplitude chattering which is due to an unavoidable measurement time-delay. The chattering problem limits the magnitude of the feedback gain while an appropriate amount of gain is required to guarantee the surface attraction condition under the existence of modeling errors. Both the "speed-density" method and the "mass-air-flow-meter" method have sufficient errors which force the gain to be increased.

There has been a great deal of research on transient A/F characteristics, and it is concluded that three characteristic delays are responsible for unwanted A/F ratio excursions during the transient operations [2], [12], [15], [17], [20]. These are the time-delay of the computer control system, a physical delay in the intake manifold and a physical delay of the fuel flow which results from the finite rate of evaporation of the fuel film on the intake manifold and port walls.

Recently, Baruah suggested a simulation model for the transient operation of spark-ignition four cylinder engines [3]. Matthews *et al.*, suggested an intake and engine control module (ECM) submodel and examined tip-in/tip-out behavior [20]. Hendricks *et al.* suggested a mean value engine model and observation air/fuel control techniques using their mean value model [15], [16], [18]. Chang *et al.* suggested a similar event-based observation control technique [1]. However, the success of the suggested observation control methods depends largely on the accuracy of the plant model. For example, in order to observe the engine speed, the external load on the engine has to be measured or estimated in some way.

In this paper, an observer-based fuel-injection control algorithm is suggested and the characteristics of the controller are compared with those of a production engine controller

and a sliding mode controller. The suggested controller is implemented on an 3.8-L V-6 engine using a PC-386.

II. Mathematical Model

For the purpose of designing a fuel-injection controller, a two-state continuous-time (mean value) engine model is used which was developed by Cho *et al.* and revised by Choi and Hedrick [7], [11], [21]. The air flow through the intake manifold can be expressed as

$$\dot{m}_a = \dot{m}_{ai} - \dot{m}_{ao}(\omega_e, m_a) \tag{1}$$

where m_a is the mass of air in the intake manifold, ω_e is the engine speed, $\dot{m}_{ai}$ is the air-mass-flow rate into the manifold, and $\dot{m}_{ao}$ is the air-mass-flow rate out of the manifold given as a function of ω_e and m_a. Since the mean value engine model is considered, $\dot{m}_{ao}$ also means the averaged air flow rate which is independent of each cylinder event. This mean value model coincides with the fact that the fuel is injected into each cylinder only once per two crank shaft rotations.

We assume a first-order perfect fuel delivery model with all the uncertainties put on the air flow model, then

$$\dot{m}_{fo} = \frac{1}{s/\tau_f + 1}\,\dot{m}_{fc} \tag{2}$$

$$\dot{m}_{ao} = (1+e)\hat{\dot{m}}_{ao}(m_a, \omega_e) \tag{3}$$

where $\dot{m}_{fc}$ is the fuel command, $\dot{m}_{fo}$ the delivered fuel, τ_f the fueling time constant, $\hat{\dot{m}}_{ao}$ the model of $\dot{m}_{ao}$, and the modeling error e is assumed to have a magnitude less than one.

Let us express (3) more generally as

$$x(t) = [1 + e(t)]\hat{x}(t) \tag{4}$$

for a model $\hat{x}(t)$ and a multiplicative time varying error $e(t)$, and let the measurement be defined as

$$y(t) = \text{sign}[x(t - t_d) - \beta u(t - t_d)] \tag{5}$$

where β is a constant, t_d is the time-delay, u is an input, and sign is a signum function. The control objective is to keep $x(t) = \beta u(t)$. In the case of fuel injection control, $u = \dot{m}_{fo}$. Assume that $\dot{x}(t)$ and $\dot{\hat{x}}(t)$ can be expressed as

$$\dot{x} = [1 + e]f(x) + g(e) \tag{6}$$

$$\dot{\hat{x}} = f(x) + \hat{g} \tag{7}$$

where

$\hat{g} = g(0)$;

$f(x)$ is monotonically decreasing about x, i.e., $\partial f/\partial x < 0$;

$|e| \le e_1 < 1$.

Note that $\partial f/\partial x = -\partial \hat{\dot{m}}_{ao}/\partial m_a$ for S.I. engines and $\partial \hat{\dot{m}}_{ao}/\partial m_a$ is always positive [9].

III. Sliding Mode Control

The sliding mode control method has been developed as a systematic way to design a controller for a nonlinear plant [22], [24]. Moreover, the binary nature of the measurement signal is in good agreement with that of the sliding mode control method.

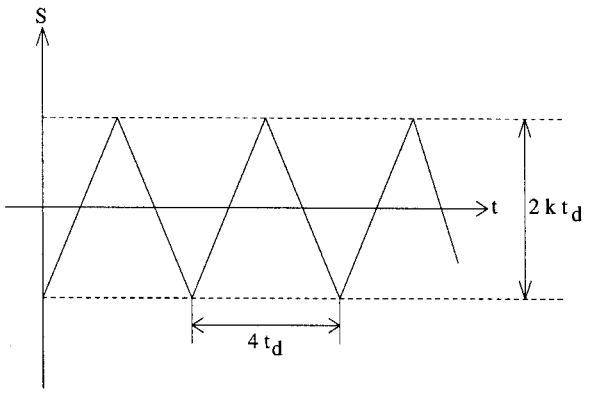

Fig. 1. Error dynamics of a sliding mode control for time-delayed feedback.

A. A Plant Without Measurement Time-Delay

As defined in Section II, the objective of controller design is to keep $x(t) = \beta u(t)$ under the existence of modeling errors and time-delay. Let the sliding surface $s(t)$ be defined as

$$s(t) \triangleq x(t) - \beta u(t) \tag{8}$$

then the control objective is $s(t) \to 0$. The $s \triangleq 0$ condition is guaranteed if $s\dot{s}$ is negative definite. A possible way to accomplish this is by choosing a control input $u(t)$ such that the attraction condition

$$s\dot{s} \le -\eta|s|, \qquad \eta > 0 \tag{9}$$

is satisfied. Since $\text{sign}[s(t - t_d)] = y(t)$, neglecting time-delay and substituting (5) and (8) into (9)

$$(1+e)\dot{\hat{x}} + \dot{e}\hat{x} - \beta\dot{u} = -\eta y. \tag{10}$$

Define the control law

$$\dot{u}_1 \triangleq \dot{u} = \frac{1}{\beta}[\dot{\hat{x}} + ky] \tag{11}$$

with

$$k > |e\dot{\hat{x}} + \dot{e}\hat{x}| \tag{12}$$

then the attraction condition of the $s = 0$ manifold is satisfied. Considering (4), (6), and (7), (11), and (12) can also be written as

$$\dot{u}_1 = \frac{1}{\beta}[f(x) + \hat{g} + ky] \tag{13}$$

$$k > |ef(x) + \tilde{g}|, \qquad \tilde{g} \triangleq g - \hat{g}. \tag{14}$$

B. The Effect of Time-Delay

Under the existence of a measurement time-delay, neglecting the modeling error term, the sliding surface equation becomes

$$\dot{s}(t) = -k\,\text{sign}[s(t - t_d)] \tag{15}$$

and the attractiveness of the surface defined by $s(t) = 0$ is not guaranteed. As shown in Fig. 1, the surface $s(t)$ chatters with the amplitude of $2kt_d$ and the frequency of $1/(4t_d)$ [6]. Since the chattering magnitude increases proportional to the gain k and the time-delay t_d, in some cases, it is not possible to choose k such that $|s| < \varepsilon$ for a desired error bound ε.

IV. Other Control Methods

As it is commented in Section III-B, the time-delay causes the problem of chattering. Using a saturation function $\mathrm{sat}(s)$ or s instead of $\mathrm{sign}(s)$ gives

$$\dot{s}(t) = -k\,\mathrm{sat}[s(t-t_d)] \tag{16}$$

or

$$\dot{s}(t) = -ks(t-t_d). \tag{17}$$

The solutions of (16) and (17) satisfy the attraction condition if $kt_d < \pi/2$. However, we can not design a controller which satisfies (16) or (17), since the magnitude of s is not available in the given plant. Therefore the following control methods are considered.

A. Parameter Adaptation

Roughly speaking, the feedback gain k is proportional to the modeling error e. If e can be made small by parameter adaptation, k can be made small too. However, in some plants, it is very hard to figure out the structure of the error to apply this method; if a plant model is composed of tables which include modeling errors and the entries at arbitrary positions are used for control, then the error is an arbitrary function of time, and conventional parameter adaptation techniques cannot be applied.

B. Gain Scheduling

The feedback gain can be varied such that

$$k(t) = |e|_{\max}\,|\dot{\hat{x}}(t)| + |\dot{e}|_{\max}\,|\hat{x}(t)| \tag{18}$$

which always satisfies the condition given in (12). However, this cannot reduce the chattering in all cases since if $|\dot{\hat{x}}|$ or $|\hat{x}|$ is large then $k(t)$ can be very large around $s \approx 0$.

C. Future Output Estimation

If $\mathrm{sign}[x(t) - \beta u(t)]$ can be estimated from $y(\tau), 0 \le \tau < t$, the problem of chattering can be solved. However, the discontinuity of $y(t)$ makes the estimation very difficult; $y(t)$ can be smoothed by filtering, but filtering causes more phase lag.

V. Observer-Based Control

The following observer-based controller is suggested to get $\dot{s} \approx -ks$ without measuring the magnitude of s. It reduces chattering due to time-delay. This can be considered to be an indirect feedback sliding mode controller or alternatively an open-loop controller based on a sliding observer. We define an observer and a control input as

$$\dot{z} = f(z) + \hat{g} + ly, \qquad l > 0 \tag{19}$$

$$u_2(t) \triangleq u(t) = \frac{1}{\beta}\, z(t) \tag{20}$$

then

$$\begin{aligned} s(t) &\triangleq x(t) - \beta u_2(t) \\ &= x(t) - z(t). \end{aligned} \tag{21}$$

Differentiating (21) and substituting (6) and (19) yields

$$\dot{s} = f(x) - f(z) - ly + ef(x) + \tilde{g}. \tag{22}$$

A. A Plant Without Time-Delay

Without measurement time-delay, $y(t) = \mathrm{sign}[s(t)]$ (as in Section III-A) and (22) becomes

$$\dot{s} = f(x) - f(z) - l\,\mathrm{sign}(s) + ef(x) + \tilde{g}. \tag{23}$$

Since $f(x)$ is monotonically decreasing about x

$$\begin{aligned} f(x) - f(z) &= -\mathrm{sign}(x-z)|f(x) - f(z)| \\ &= -\mathrm{sign}(s)|f(x) - f(z)|. \end{aligned} \tag{24}$$

Substituting (24) into (23), the error dynamic equation becomes

$$\dot{s} = -[|f(x) - f(z)| + l]\,\mathrm{sign}(s) + ef(x) + \tilde{g}. \tag{25}$$

Here, from the monotonicity of f with respect to its argument, $|f(x) - f(z)| + l$ is large for large s and small for small s as ks ($k > 0$) is. This means fast tracking with small chattering around $s \approx 0$. Now, define the feedback gain l such that

$$l > |ef(z) + \tilde{g}| \tag{26}$$

then, from the assumption that $|e| < 1$

$$\begin{aligned} |f(x) - f(z)| + l &> |f(x) - f(z)| + |ef(z) + \tilde{g}| \\ &\ge |ef(x) - ef(z)| + |ef(z) + \tilde{g}| \\ &\ge |ef(x) + \tilde{g}|. \end{aligned} \tag{27}$$

Therefore, from (25), the attraction condition of the $s = 0$ manifold is satisfied without additional calculation to get $f(x)$ [Note that $l = k > |ef(x) + \tilde{g}|$ also satisfies the attraction condition.] If f does not satisfy the assumption, l should be greater than k [$l > |ef(x)+\tilde{g}|+|f(x)-f(z)|$, $k > |ef(x)+\tilde{g}|$] to satisfy the attraction condition and the sliding mode control gives a solution with a smaller feedback gain.

B. The Effect of Time-Delay

The effect of measurement time-delay is considered and the effect on the observer-based control is compared to that on the sliding mode control of Section III-B, when they have the same feedback gains ($l = k$) and $f(x)$ is a linear function, i.e.,

$$f(x) = -ax, \qquad a > 0. \tag{28}$$

Neglecting the modeling error terms, the time-delayed tracking error dynamic equation becomes

$$\dot{s}(t) = -as(t) + k\,\mathrm{sign}[s(t-t_d)]. \tag{29}$$

For $0 \le t \le 2t_d$ with $s(0) = -|s|_{\max}$, the analytical solution of (29) is

$$s(t) = \frac{k}{a}\,\frac{1 + \exp(-2at_d) - 2\exp(-at)}{1 + \exp(-2at_d)}. \tag{30}$$

The chattering magnitude of this control is $2k[1 - \exp(-2at_d)]/a[1 + \exp(-2at_d)]$ which is always less than that of the equivalent sliding control ($2kt_d$) for any $a > 0$ and t_d (See Figs. 1 and 2).

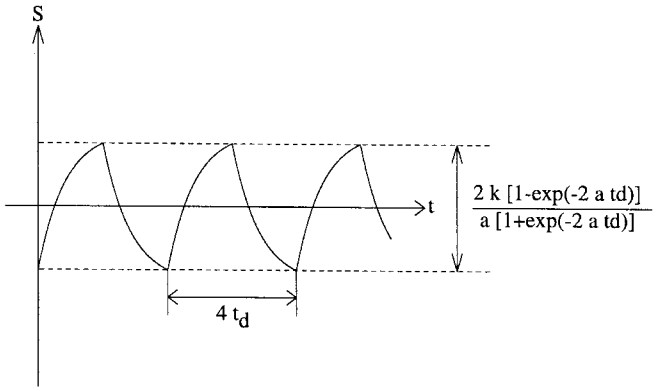

Fig. 2. Error dynamics of an observer-based control for time-delayed feedback.

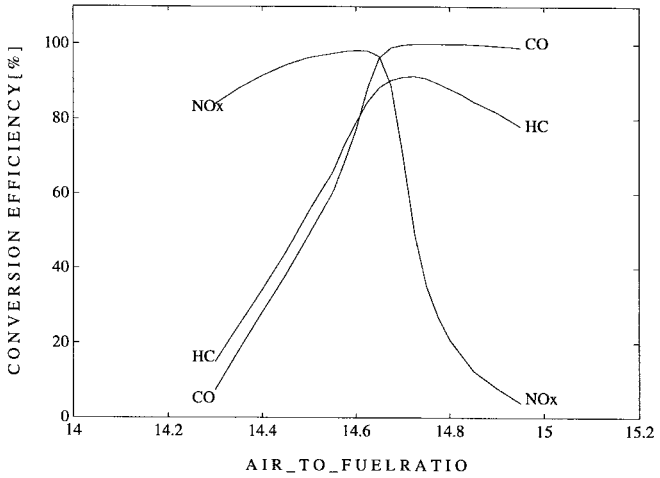

Fig. 3. A typical catalytic converter efficiency (adapted from [14]).

C. Optimal Gain

In Section V-B, it has been shown that the chattering magnitude of the observer-based control is less than that of the sliding mode control for the same feedback gains. Further, an optimal feedback gain can be found which makes the magnitude much less. Assume that f is linear and given by (28).

In (25), $|s|$ is bounded by the relation

$$\begin{aligned} |f(x)-f(z)|+l &= a|s|+l \\ &= |ef(x)+\tilde{g}| \\ &\triangleq e^*. \end{aligned} \tag{31}$$

Equivalently

$$|s|_{\max}=\frac{1}{a}(e^*-l). \tag{32}$$

Also, from (30) with the gain l substituted for k, the chattering magnitude due to the time-delay is

$$|s|_{\max}=\frac{l}{a}\frac{1-\exp(-2at_d)}{1+\exp(-2at_d)}. \tag{33}$$

Equating (32) and (33), the optimal gain l which minimize $|s|_{\max}$ is

$$l_{opt}=\frac{e^*}{2}[1+\exp(-2at_d)] \tag{34}$$

and the equivalent maximum chattering magnitude

$$|s|_{\max,\,opt}=\frac{e^*}{2a}[1-\exp(-2at_d)]. \tag{35}$$

So, if $a=20$ and $t_d=0.12$ which are the typical values in a fuel-injection system, the chattering magnitude can be reduced to 1/5 of that of the sliding mode control.

VI. Application to Air-to-Fuel Ratio Control

The most important objective of fuel-injection control is to keep the A/F ratio close to a stoichiometric ratio ($\beta=14.7$) so as to maximize the efficiency of the three-way catalyst. As shown in Fig. 3, the steady-state conversion efficiency of the catalyst is very sensitive to the variation of the ratio, and even 1% deviation from the stoichiometric ratio results in up to 50% degradation in the conversion of one or more pollutants. Thus, the objective of the control is to keep the A/F ratio at 14.7 : 1 very strictly. However, a slow and very small magnitude oscillation of the A/F ratio improves the conversion efficiency [6].

Since the control objective is keeping the A/F ratio constant, we can put the model error either in the air flow model or the fuel flow model. For ease of analysis, we put all the modeling errors are put on the air flow model and a perfect fuel delivery model is assumed. In the process of designing the controllers, the measurement time-delay is neglected. In this section, a two-state engine model is used, and the sliding mode controller and the observer-based controller are compared.

A. Engine Model

Consider the engine model given in (1)–(3). Differentiating (3) and substituting into (1)

$$\begin{aligned} \underbrace{\ddot{m}_{ao}}_{\dot{x}} &= (1+e)\underbrace{\left(-\frac{\partial\dot{\hat{m}}_{ao}}{\partial m_a}\dot{m}_{ao}\right)}_{f(x)} \\ &\quad \underbrace{+(1+e)\left(\frac{\partial\dot{\hat{m}}_{ao}}{\partial m_a}\dot{m}_{ai}+\frac{\partial\dot{\hat{m}}_{ao}}{\partial\omega_e}\dot{\omega}_e\right)+\dot{e}\dot{\hat{m}}_{ao}}_{g}. \end{aligned} \tag{36}$$

Here

$$\frac{\partial f(x)}{\partial x}=-\frac{\partial\dot{\hat{m}}_{ao}}{\partial m_a}<0 \tag{37}$$

for all spark ignition engines [9]. So the assumption about $f(x)$ is satisfied. The partial derivatives are the slope of the mean-value engine model $\dot{\hat{m}}_{ao}$ with respect to its arguments. Normally, $\dot{\hat{m}}_{ao}$ is obtained empirically, and the derivatives are observed to be almost constant. The measurement output of a binary oxygen sensor is

$$y(t)=\operatorname{sign}[\underbrace{\dot{m}_{ao}(t-t_d)}_{x(t-t_d)}-\beta\underbrace{\dot{m}_{fo}(t-t_d)}_{u(t-t_d)}]. \tag{38}$$

B. Sliding Mode Control

Define a sliding surface [8], [9]

$$s \triangleq \dot{m}_{ao} - \beta \dot{m}_{fo} \tag{39}$$

and apply the attraction condition [19]

$$\dot{s} = -k \operatorname{sign}(s). \tag{40}$$

Substituting (1) and (36) into (40)

$$\begin{aligned} \ddot{m}_{fo1} \triangleq \ddot{m}_{fo} = \frac{1}{\beta}\left(\frac{\partial \dot{\hat{m}}_{ao}}{\partial m_a}\dot{m}_a + \frac{\partial \dot{\hat{m}}_{ao}}{\partial \omega_e}\dot{\omega}_e\right) \\ + \frac{e}{\beta}\left(\frac{\partial \dot{\hat{m}}_{ao}}{\partial m_a}\dot{m}_a + \frac{\partial \dot{\hat{m}}_{ao}}{\partial \omega_e}\dot{\omega}_e\right) \\ + \frac{\dot{e}}{\beta}\dot{\hat{m}}_{ao} + \frac{k}{\beta}\operatorname{sign}(s). \end{aligned} \tag{41}$$

Therefore, the attraction condition of the $s = 0$ manifold is satisfied if

$$\ddot{m}_{fo1} = \frac{1}{\beta}\left(\frac{\partial \dot{\hat{m}}_{ao}}{\partial m_a}\dot{m}_a + \frac{\partial \dot{\hat{m}}_{ao}}{\partial \omega_e}\dot{\omega}_e\right) + \frac{k}{\beta}\operatorname{sign}(s) \tag{42}$$

and

$$k = |e|_{\max}\left|\frac{\partial \dot{\hat{m}}_{ao}}{\partial m_a}\dot{m}_a + \frac{\partial \dot{\hat{m}}_{ao}}{\partial \omega_e}\dot{\omega}_e\right| + |\dot{e}|_{\max}\dot{\hat{m}}_{ao}. \tag{43}$$

Integrating (42), the control law

$$\dot{m}_{fo1}(t) = \frac{1}{\beta}\dot{\hat{m}}_{ao}(t) + \frac{1}{\beta}\int_0^t ky(\tau)\,d\tau \tag{44}$$

and the actual fuel command $\dot{m}_{fc}$ can be obtained from (2).

C. Observer-Based Control

Define an observer and an input as

$$\dot{z} = -\frac{\partial \dot{\hat{m}}_{ao}}{\partial m_a}z + \frac{\partial \dot{\hat{m}}_{ao}}{\partial m_a}\dot{m}_{ai} + \frac{\partial \dot{\hat{m}}_{ao}}{\partial \omega_e}\dot{\omega}_e + ly \tag{45}$$

$$\dot{m}_{fo2}(t) \triangleq \dot{m}_{fo} = \frac{1}{\beta}z(t). \tag{46}$$

Subtracting (45) from (36) and plugging in (1)

$$\begin{aligned} \ddot{m}_{ao} - \dot{z} = -\frac{\partial \dot{\hat{m}}_{ao}}{\partial m_a}(\dot{m}_{ao} - z) - ly + \dot{e}\dot{\hat{m}}_{ao} \\ + e\left(\frac{\partial \dot{\hat{m}}_{ao}}{\partial m_a}\dot{m}_a + \frac{\partial \dot{\hat{m}}_{ao}}{\partial \omega_e}\dot{\omega}_e\right). \end{aligned} \tag{47}$$

Define s as in (39) and choose

$$\begin{aligned} l = |e|_{\max}\left|\frac{\partial \dot{\hat{m}}_{ao}}{\partial m_a}(\dot{m}_{ai} - \beta\dot{m}_{fo2}) + \frac{\partial \dot{\hat{m}}_{ao}}{\partial \omega_e}\dot{\omega}_e\right| \\ + |\dot{e}|_{\max}\dot{\hat{m}}_{ao} \end{aligned} \tag{48}$$

or $l = k$ as that obtained in (43) then (47) becomes

$$\begin{aligned} \dot{s} = -\left(\frac{\partial \dot{\hat{m}}_{ao}}{\partial m_a}|s| + l\right)\operatorname{sign}(s) \\ + e\left(\frac{\partial \dot{\hat{m}}_{ao}}{\partial m_a}\dot{m}_a + \frac{\partial \dot{\hat{m}}_{ao}}{\partial \omega_e}\dot{\omega}_e\right) + \dot{e}\dot{\hat{m}}_{ao} \end{aligned} \tag{49}$$

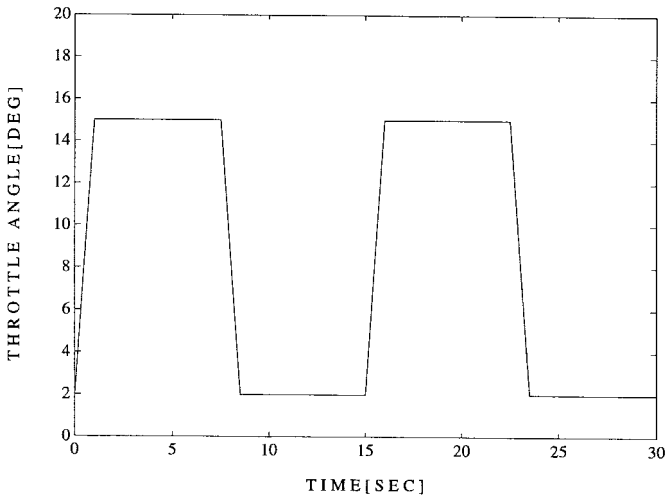

Fig. 4. Throttle changes for a simulation.

and the attraction condition is satisfied. Under the existence of the measurement time-delay, the gain l_{opt} can be chosen which minimizes the chattering from (34). Integrating (45), the control law

$$\begin{aligned} \dot{m}_{fo2}(t) = \dot{m}_{fo2}(0) + \frac{1}{\beta}\int_0^t \\ \cdot\left\{\frac{\partial \dot{\hat{m}}_{ao}}{\partial m_a}[\dot{m}_{ai} - \beta\dot{m}_{fc2}(\tau)] + \frac{\partial \dot{\hat{m}}_{ao}}{\partial \omega_e}\dot{\omega}_e\right\}d\tau \\ + \frac{1}{\beta}\int_0^t ly(\tau)\,d\tau. \end{aligned} \tag{50}$$

This control law shows a good way to combine the speed-density method which uses $\dot{\hat{m}}_{ao}$ (ω_e and m_a need to be measured to get $\dot{\hat{m}}_{ao}$) and the air-mass-flow-meter method which uses $\dot{m}_{ai}$ efficiently.

VII. Simulation Results

Since the model error is unknown, the error is assumed as follows:

$$e(t) = 0.1\sin(\pi t). \tag{51}$$

This represent $\pm 10\%$ error with 0.5 Hz frequency which is five times faster than the error model used in [6]. Even though this assumed error is quite different from the real one, it is used to compare the response of the developed control laws by simulation.

The measurement time-delay of the oxygen sensor is the transportation time for an amount of air to enter the cylinders, go through combustion, and travel down to the sensor plus sensor response time. In this paper, $t_d = 20$ ms $+ 4\pi/\omega_e(t)$ was chosen for simulation [6]. The throttle is varied as shown in Fig. 4 to simulate fast acceleration and deceleration which allows the engine to be operated between 1000 and 4000 r/min (see Fig. 5).

First, the performance of the sliding mode controller was demonstrated for the case with modeling error but without measurement time-delay. The simulation result is as shown in Fig. 6 and the performance is very good as expected. However,

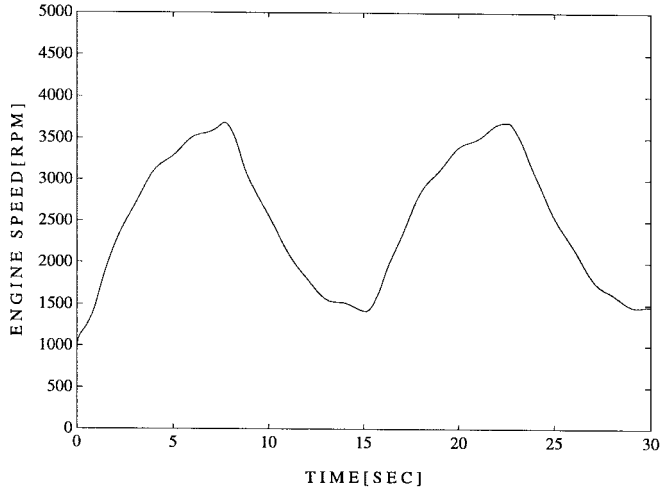

Fig. 5. Engine speed changes: simulation.

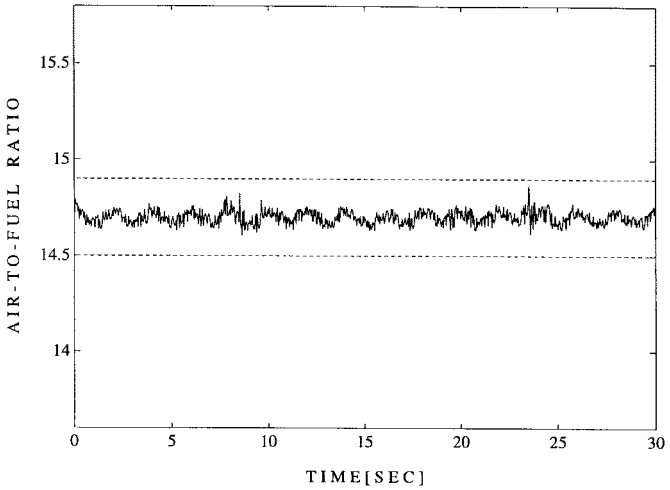

Fig. 6. A/F ratio for the sliding mode control: no measurement time-delay, gain $= k$.

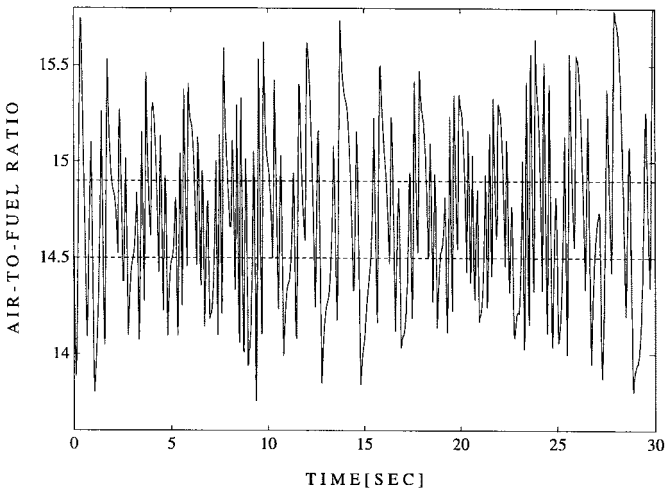

Fig. 7. A/F ratio for the sliding mode control: with measurement time-delay, gain $= k$.

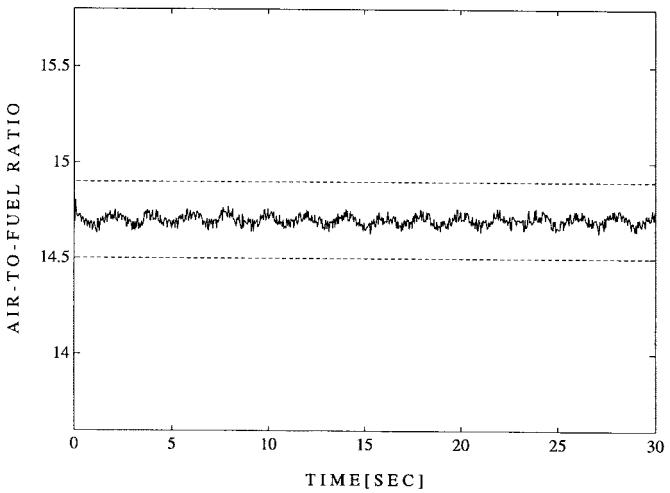

Fig. 8. A/F ratio for the observer-based control: no measurement time-delay, gain $= k$.

under the existence of the time-delay, the performance is deteriorated very much as shown in Fig. 7.

Second, the performance of the observer-based controller was demonstrated for the case with modeling error but without measurement time-delay. The simulation result is as shown in Fig. 8 and the performance is very good as in the case of the sliding mode control. Next, the observer-based control was simulated for the plant with the time-delay and the feedback gain is 1/2 that of the sliding mode control, since the optimal gain is approximately 1/2 of the regular one when the time-delay is considerably large. Fig. 9 shows that this controller is very robust to the time-delay and the A/F ratio is in the desired boundary of $\pm 1.4\%$ error for most of the time.

VIII. Experimental Results

Most of the experimental results reported in the literature are obtained for tip-in tip-out throttle modes but for a fixed engine speed. However, in many cases, the engine speed changes dramatically during the quick throttle modes, since such throttle modes generally accompany gear shifting. Other results are obtained when the tip-in tip-out modes are in the large throttle opening zone. Since the intake manifold air pressure (or air mass) reaches more than 80% of the atmospheric (or full-open throttle) pressure before the throttle is half-opened, the severe throttle modes in the large throttle opening zone give only mild variations of the manifold pressure.

In this study, all the experimental results are obtained under more severe and more realistic conditions; the dynamometer load is fixed, dynamometer inertia is the only external inertia, the throttle varies in a small throttle opening zone. To emphasize these points, all the experimental results accompany the plots of the throttle and the engine speed variations.

The suggested controller was evaluated at the University of California Berkeley engine dynamometer test rig, and compared with a production ECM and a sliding mode controller.

The engine used for the test is a 3.8-L V-6 sequential port-injection S.I. engine, so the controllers were implemented in the same manner. The controllers were implemented using a 33-MHz-CPU PC-386 and a MicroSoft Quick-C compiler at 5-ms loop-time, and premium gasoline was used. The throttle

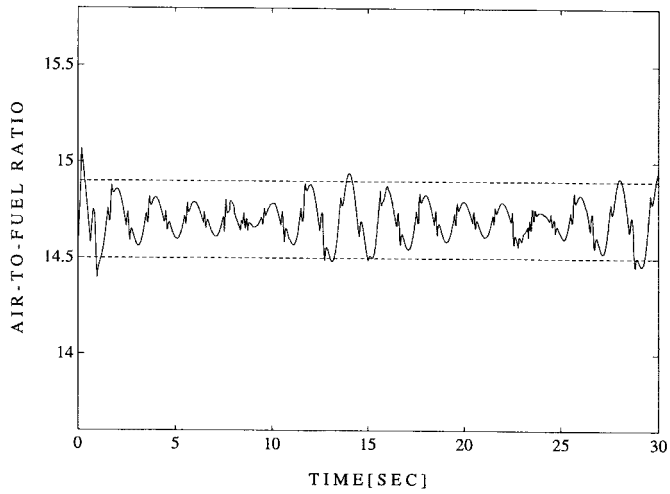

Fig. 9. A/F ratio for the observer-based control: with measurement time-delay, gain $= k/2$.

was controlled by a stepper motor which has a maximum speed of 900 steps/s and a motor controller which allows the throttle to be changed stepwise abruptly in less than 0.1 s. The fuel injector driver was built using six LM322N timer chips which modulate the injection pulse width from the production ECM when it is needed to run the observer-based controller or the sliding mode controller. The air-mass-flow rate through the throttle body, the manifold air mass, pressure, and temperature and the oxygen in the exhaust gas were measured using typical production engine sensors. The engine speed was measured by using a magnetic pick-up installed on the engine fly wheel. A linear oxygen sensor (NISSAN model PLR-1) installed in the exhaust pipe was used only to monitor the A/F ratio, and a binary oxygen sensor was used in the controls.

First, the production ECM was tested in open-loop with the throttle changed as in Fig. 10(a) and the dynamometer load fixed to 67.7 N-m. Fig. 10(c) shows that there exist large offset errors in the A/F ratio and the transient response is very slow.

Next, the ECM was tested in closed loop for the same conditions as above. Fig. 11 shows that, the offset errors are reduced considerably but there exist very large and slow transient excursions of the A/F ratio. The excursions were observed frequently even at the steady-state operation of the engine. The excursions were reduced by testing the same throttle mode repeatedly, but the steady-state chattering of the A/F ratio was unavoidable which is due to the time-delay between fueling and oxygen sensing.

Fig. 12 shows the results of the sliding mode control when the oxygen sensor signal was fed back. The sliding mode controller depends heavily on the lookup table of $\dot{m}_{ao}$ which is a function of m_a and ω_e. In addition to the oxygen sensor time-delay, this controller has a problem of sensitivity to sensor noise. As the figure shows, there are large A/F ratio excursions at some region where $\dot{m}_{ao}$ has large errors (the table of $\dot{m}_{ao}$ used in this test has large modeling errors at the region where ω_e is greater than 3000 r/min).

Fig. 13 shows the results of the observer-based control given in (50) when the oxygen sensor signal was fed back. The controller uses $\partial\dot{\hat{m}}_{ao}/\partial m_a(\omega_e, m_a)$ and $\partial\dot{\hat{m}}_{ao}/\partial\omega_e(\omega_e, m_a)$

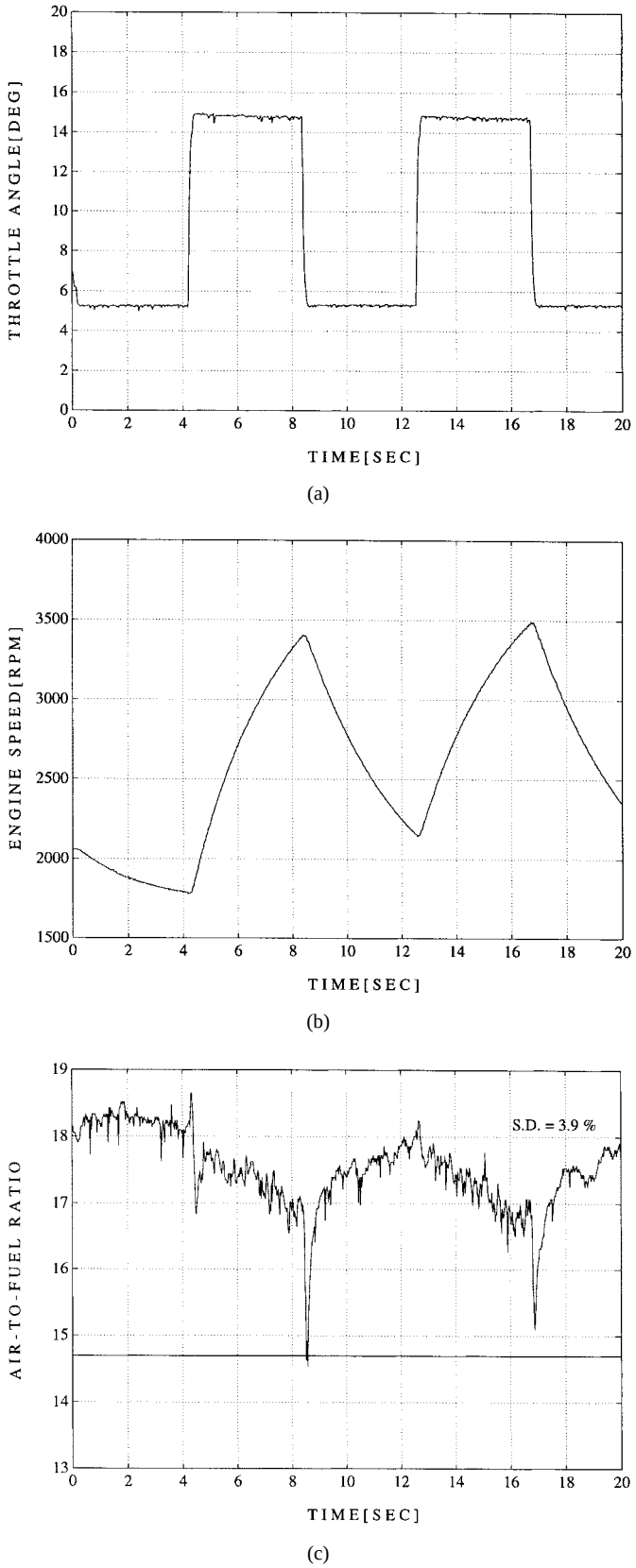

Fig. 10. Product ECM: open-loop control.

which are obtained numerically from $\dot{\hat{m}}_{ao}$ and very insensitive to the variation of the arguments, $\dot{m}_{ai}$ which has relatively less error and time-delay and $\dot{\omega}_e$ which is obtained numerically

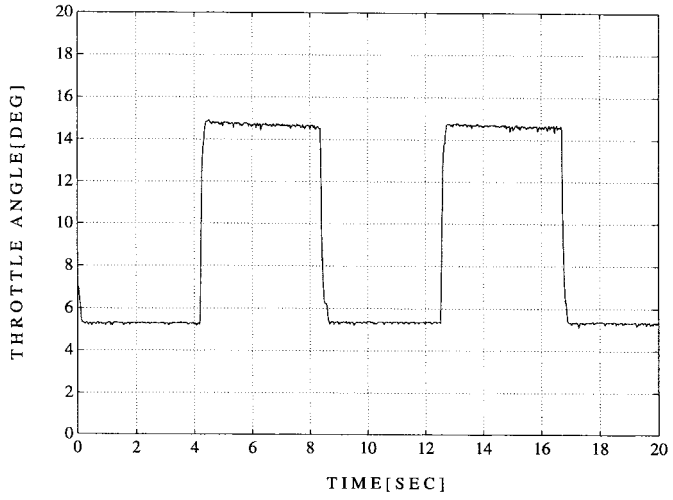

(a)

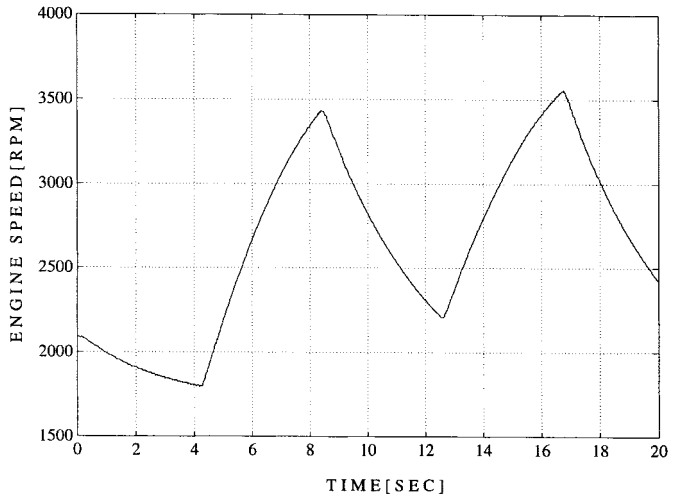

(b)

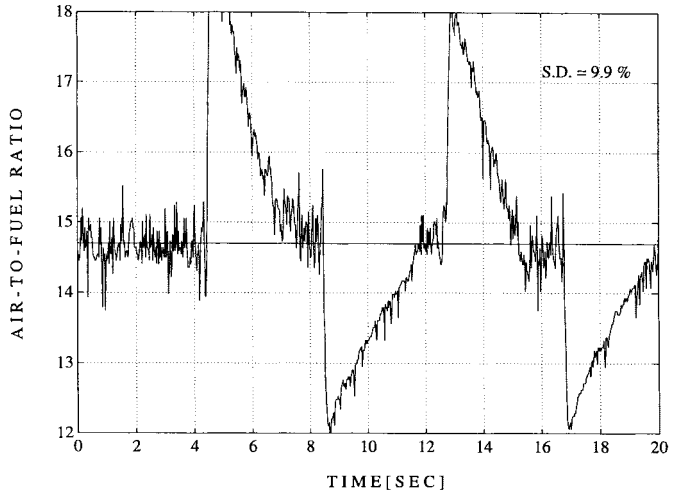

(c)

Fig. 11. Product ECM: closed-loop control.

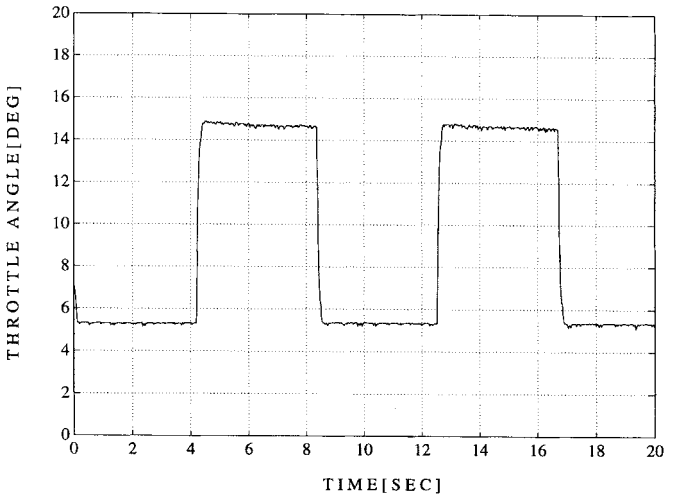

(a)

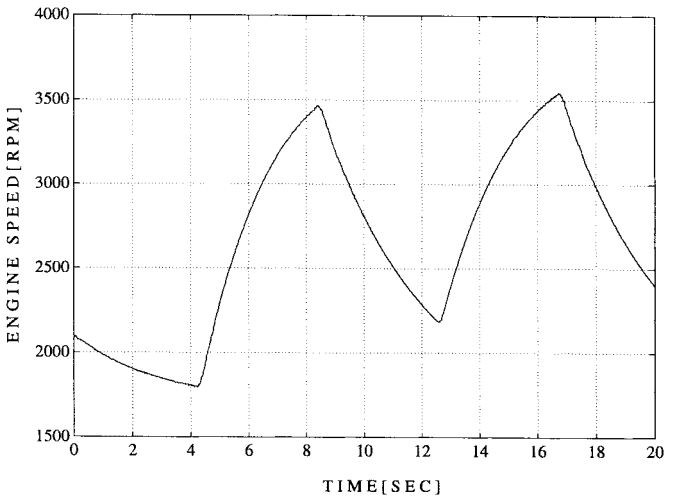

(b)

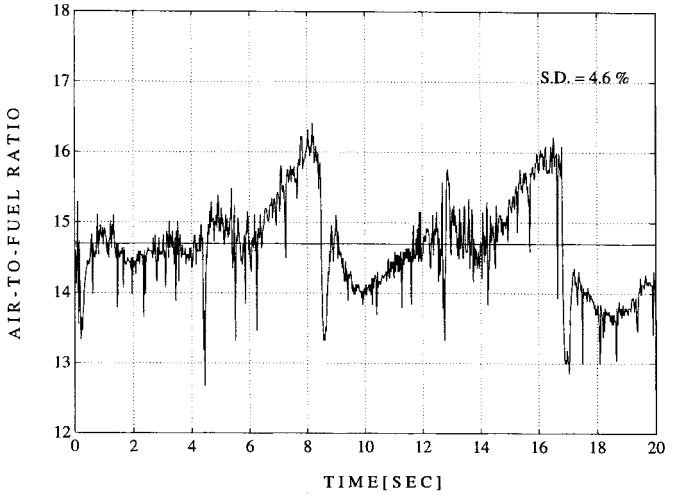

(c)

Fig. 12. Sliding mode control: closed-loop.

from ω_e having some noise and time-delay. However, they do not cause much of a problem since ω_e varies very slowly compared to other values like the throttle and the manifold air pressure and only the integrated value of $\dot{\omega}_e$ is used for control. The results show that this controller surpasses the production ECM.

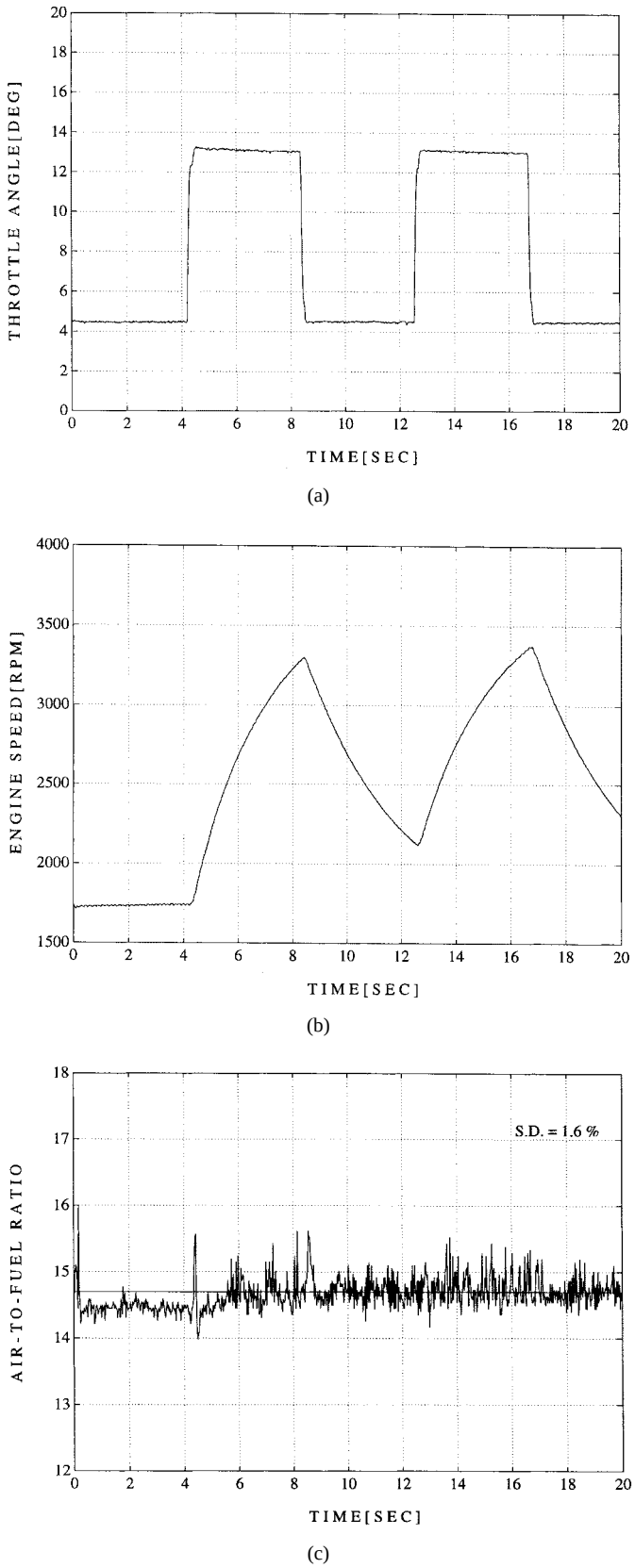

Fig. 13. Observer-based control: closed-loop.

We have assumed a first-order fuel delivery model with the time constant τ_f fixed (2). The small transient excursions in Fig. 13 are caused partly by this simple model and better transient response may be expected by scheduling τ_f or using a better fuel delivery model [20]. Even with this very simple fuel delivery model, the experimental results show that the observer-based controller reduces the chattering magnitude considerably, responds very fast to a throttle change, and is robust to modeling and sensing errors.

IX. Conclusion

In spite of many good features of sliding mode control, implementing the sliding controller directly for fuel-injection control has the problem of a large chattering magnitude due to the measurement time-delay. The problem was solved by implementing the suggested observer-based controller. If f does not satisfy the required condition ($\partial f/\partial x < 0$), the sliding mode control is the better solution. However, if f satisfies the condition and the slope of f is large, the observer-based controller has much better performance. The slope in a the fuel-injection system ($-\partial \hat{m}_{ao}/\partial m_a$) is very large ($\approx -20$), and the observer-based controller has been shown to be robust to the time-delay and stable for abruptly changing driving conditions while reducing the chattering magnitude considerably.

Acknowledgment

The authors thank P. Devlin of the California PATH program for his assistance in building the control devices for the experimental validation.

References

[1] A. Amstutz, N. P. Fekete, and J. D. Powell, "Model based air-fuel ratio control in SI engines with a switch-type EGO sensor," SAE Paper 940972, 1994.
[2] C. F. Aquino, "Transient A/F control characteristics of the five-liter central fuel injection engine," SAE Paper 810494, 1981.
[3] P. C. Baruah, "A simulation model for transient operation of spark-ignition engines," SAE Paper 900682, 1990.
[4] R. Canale *et al.*, "General motors phase II catalyst system," SAE Paper 780205, 1978.
[5] J. F. Cassidy, M. Athans, and W.-H. Lee, "On the design of electronic automotive engine controls using linear quadratic control theory," *IEEE Trans. Automat. Contr.*, vol. AC-25, Oct. 1980.
[6] D. Cho and J. K. Hedrick, "A nonlinear controller design method for fuel-injected automotive engines," *ASME Trans. J. Engine, Gas Turbines, and Power*, July 1988.
[7] ——, "Automotive powertrain modeling for control," *Trans. ASME Dynamic Syst., Measurement, Contr.*, vol. 111, Dec. 1989.
[8] ——, "Sliding mode fuel-injection controller: Its advantages," *ASME J. Dynamic Syst., Measurement, Contr.*, vol. 113, no. 3, pp. 537–541, Sept. 1991.
[9] S. B. Choi, "Design of a robust controller for automotive engines: Theory and experiment," Ph.D. dissertation, Univ. California, Berkeley, Dec. 1993.
[10] S. B. Choi and J. K. Hedrick, "An observer-based controller design method for improving air/fuel characteristics of S.I. engines: Theory and experiment," in *ASME WAM, Symp. Transportation Syst.*, 1993.
[11] ——, "Sliding control of automotive engines: Theory and experiment," *ASME WAM, Symp. Transportation Syst.*, vol. DSC-44, 1992.
[12] D. J. Dobner, "A mathematical engine model for development of dynamic engine control," SAE Paper 800054, 1980.
[13] J. C. Doyle and G. Stein, "Multivariable feedback design: Concepts for a classical/modern synthesis," *IEEE Trans. Automat. Contr.*, vol. AC-26, Feb. 1981.
[14] C. D. Falk and J. J. Mooney, "Three-way conversion catalysts: Effect of closed-loop feedback control and other parameters on catalyst efficiency," SAE Paper 800462, 1980.
[15] E. Hendricks and T. Vesterholm, "The analysis of mean value SI engine models," SAE Paper 920682, 1992.

[16] E. Hendricks, T. Vesterholm, and C. Sorenson, "Nonlinear closed-loop SI engine control observers," SAE Paper 920237, 1992.
[17] S. D. Hires and M. T. Overington, "Transient mixture strength excursions—An investigation of their causes and the development of a constant mixture strength fueling strategy," SAE Paper 810495, 1981.
[18] P. Kaidantzis, P. Pasmussen, M. Jensen, T. Vesterholm, and E. Hendricks, "Advanced nonlinear observer control of SI engines," in *SAE Annu. Meet.*, 1993.
[19] K. Allen, "Nonlinear control methods for automotive engines," M.S. thesis, Massachusetts Inst. Technol., Cambridge, June 1986.
[20] R. D. Matthews *et al.*, "Intake and ECM submodel improvements for dynamic SI engine models: Examination of tip-in/tip-out," SAE Paper 910074, 1991.
[21] J. J. Moskwa and J. K. Hedrick, "Modeling and validation of automotive engines for control algorithm development," *ASME WAM, Advanced Automotive Technol.*, vol. DSC-13, 1989.
[22] J. J. E. Slotine and W. Li, *Applied Nonlinear Control.* Englewood Cliffs, NJ: Prentice-Hall, 1991.
[23] Y. Sogawa *et al.*, "Improvement of engine transient characteristics using an induction chamber model," *Int. J. Vehicle Design*, vol. 10, no. 5, 1989.
[24] V. I. Utkin, *Sliding Modes and Their Application in Variable Structure System*, translated by A. Parnakh. Moscow: MIR, 1978.

Seibum B. Choi received the B.S. degree in mechanical engineering from Seoul National University, Seoul, Korea, in 1985, and the M.S. degree in mechanical engineering from Korea Advanced Institute of Science and Technology, Seoul, Korea, in 1987. From 1990 to 1993, he was at the University of California, Berkeley (UCB) where he received the Ph.D. degree in controls.

From 1993 to 1997, he was working for the development of Automated Vehicle Control Systems at Institutes of Transportation Studies of UCB. Currently, he is with Varity Kelsey-Hayes, MI, working on vehicle braking systems.

J. Karl Hedrick received the Ph.D. degree from Stanford University, CA.

He is the James Marshall Wells Professor of Mechanical Engineering at the University of California, Berkeley. He is currently the Director of the California PATH Research Center. He taught at Arizona State University, Tempe, and Massachusetts Institute of Technology, Cambridge, before coming to UC Berkeley in 1988. His areas of research and teaching are in nonlinear control theory and advanced vehicle control systems.

Dr. Hedrick is a Fellow of ASME and Editor of the *Vehicle System Dynamics Journal*.